CERKL gene knockout disturbs photoreceptor outer segment phagocytosis and causes rod-cone dystrophy in zebrafish

Yu, Shanshan ; Li, Chang; Biswas, Lincoln; Hu, Xuebin; Liu, Fei; Reilly, James; Liu, Xiliang; Liu, Ying ; Huang, Yuwen; Lu, Zhaojing; Han, Shanshan; Wang, Lei; Liu, Jing Yu ; Jiang, Tao ; Shu, Xinhua; Wong, Fulton; Tang, Zhaohui ; Liu, Mugen

Published in:
Human Molecular Genetics

DOI:
10.1093/hmg/ddx137

Publication date:
2017

Document Version
Author accepted manuscript

CERKL gene knockout disturbs photoreceptor outer segment phagocytosis and causes rod-cone dystrophy in zebrafish

Shanshan Yu[1,+], Chang Li[1,+], Lincoln Biswas[2], Xuebin Hu[1], Fei Liu[1], James Reilly[2], Xiliang Liu[1], Ying Liu[1], Yuwen Huang[1], Zhaojing Lu[1], Shanshan Han[1], Lei Wang[3], Jing Yu Liu[1], Tao Jiang[1], Xinhua Shu[2], Fulton Wong[4], Zhaohui Tang[1,*], Mugen Liu[1,*]

1 Key Laboratory of Molecular Biophysics of Ministry of Education, Department of Genetics and Developmental Biology, College of Life Science and Technology, Huazhong University of Science and Technology, Wuhan, Hubei 430074, PR China.
2 Department of Life Sciences, Glasgow Caledonian University, Glasgow G4 0BA, Scotland.
3 Department of Pathology & Lab Medicine, University of Cincinnati Medical Center, Cincinnati, Ohio, 45267, USA.
4 Department of Ophthalmology, Duke University School of Medicine, Durham, NC 27710, USA.

† The authors wish it to be known that, in their opinion, the first two authors should be regarded as joint first authors

*To whom correspondence should be addressed at: Department of Genetics and Developmental Biology, College of Life Science and Technology, 1037 Luoyu Road, Wuhan, P. R. China. Tel: 86 27 87794549; Fax 86 27 87794549; Email: lium@hust.edu.cn(M.L.); zh_tang@mail.hust.edu.cn(Z.T.)

Abstract

In humans, *CERKL* mutations cause widespread retinal degeneration: early dysfunction and loss of rod and cone photoreceptors in the outer retina and, progressively, death of cells in the inner retina. Despite intensive efforts, the function of CERKL remains obscure and studies in animal models have failed to clarify the disease mechanism of *CERKL* mutations. To address this gap in knowledge, we have generated a stable *CERKL* knockout zebrafish model by TALEN technology and a 7bp deletion in *CERKL* cDNA that caused the premature termination of CERKL. These *CERKL*$^{-/-}$ animals showed progressive degeneration of photoreceptor outer segments (OSs) and increased apoptosis of retinal cells, including those in the outer and inner retinal layers. Additionally, we confirmed by immunofluorescence and western-blot that rod degeneration in *CERKL*$^{-/-}$ zebrafish occurred earlier and was more significant than that in cone cells. Accumulation of shed OSs in the interphotoreceptor matrix was observed by transmission election microscopy (TEM). This suggested that CERKL may regulate the phagocytosis of OSs by the retinal pigment epithelium (RPE). We further found that the phagocytosis-associated protein MERTK was significantly reduced in *CERKL*$^{-/-}$ zebrafish. Additionally, in ARPE-19 cell lines, knockdown of *CERKL* also decreased the mRNA and protein level of MERTK, as well as the ox-POS phagocytosis. We conclude that CERKL deficiency in zebrafish may cause rod-cone dystrophy, but not cone-rod dystrophy, while interfering with the phagocytosis function of RPE associated with down-regulation of the expression of MERTK.

Introduction

CERKL is a gene known to cause retinitis pigmentosa (RP) and was first characterized in a recessive RP Spanish family in 2004 (1). Until now twelve mutants have been reported worldwide (1–9); of particular note is the c.238 + 1G > A of *CERKL* that underlies approximately 33% of autosomal recessive retinal degeneration cases in the Yemenite Jewish population (4). Identifying the function of CERKL will help us to understand the pathological mechanisms of RP.

Human *CERKL* contains 13 exons that encode a polypeptide of 532 amino acids. The protein is a homolog of ceramide kinase (CERK), containing a Pleckstrin homology (PH) domain and an evolutionarily conserved diacylglycerol kinase (DAGK) domain (1). Accordingly, CERKL is thought to be involved in sphingophospholipid metabolism, perhaps as a ceramide kinase (10,11). However, any kinase activity of CERKL remains to be demonstrated in *in vitro* and *in vivo* assays (10,12). The subcellular location of CERKL is highly dynamic, shifting from the ER-Golgi network to the nucleus (13). In the mouse retina, the CERKL protein is prominently localized in the ganglion cell layer (GCL), inner nuclear layer (INL), retina pigment epithelium (RPE), and photoreceptor inner segments (14). In zebrafish, immunofluorescence from cryosections revealed a strong signal in the outer segment (OS) and inner segment (IS) of photoreceptors (15). The diverse cellular and subcellular localization of CERKL is accompanied by a complex pattern of mature mRNA transcripts that result from several transcriptional start sites and multiple alternative splicing events (16). Collectively, these observations suggest that CERKL is likely to have multiple functional roles in different cell types.

Though an animal model is an important tool in the investigation of the function of CERKL, the complex gene structure of CERKL in the mouse presents special challenges for the creation of genetic mouse models. To date, two mouse models of CERKL have been constructed, one of which carried a deletion of exon 5 where the most common mutation (R257X) is located, while the other abolished the first exon plus 1.2kb upstream region; both models, however, showed no gross retinal dystrophy (11,16,17).

The zebrafish model has become an excellent tool with which to investigate the mechanisms of retinal degradation, as the zebrafish retina has a similar structure - containing the same main cell types - to that of the human retina (18). Furthermore, Zebrafish *CERKL* contains 13 exons encoding a protein of 577 amino acids that share 59% identity and 82% similarity with human CERKL. Unlike the complexity of transcripts seen in mouse and human, there are only three transcripts in zebrafish; this simpler structure offers the possibility of completely removing CERKL (19). Studies in zebrafish have so far depended on transient knockdown using morpholino injection, which caused abnormal eye development and resulted in small eyes, defective retinal lamination, absence of cone and rod photoreceptors and increased apoptosis of retinal cells, in addition to markedly small head, curved body axes and short tail (19).

In this study, we constructed the *CEKRL* knockout zebrafish by TALEN technology. We identified a 7bp deletion in the CERKL exon1, which causes a frame shift resulting in complete

CERKL protein degradation. In *CERKL*$^{-/-}$ zebrafish, the disorganized OSs were observed from 2-month old, followed ultimately by photoreceptor death. A great deal of shed OSs was observed to have accumulated in the space between the OSs and RPE, suggesting that CERKL may regulate phagocytosis of OSs by the RPE. Meanwhile, we found evidence that CERKL might regulate the expression of MERTK, which plays an important role in the RPE's phagocytosis of OSs.

Results

Generation of *CERKL* mutant with TALENs

Transcription Activator-Like Effector Nuclease (TALEN), which is a new genome editing technique, has been a powerful tool for the generation of site-specific DNA double-strand breaks (DSBs) that trigger error-prone nonhomologous end joining (NHEJ) or homology-directed repair (HDR) pathway to induce insertion or deletion (indel) mutations in targeted genes, which typically results in amino acid changes or premature stop codons in the mRNA (20).

To generate a *CERKL* (NM_001089474.1) knockout (*CERKL*$^{-/-}$) zebrafish by TALEN, the target sites were designed at the first exon with the aim of inactivating the entire protein. The left and right binding sites of this TALEN were separated by a 18-bp spacer containing a Mlu1 digest site (Fig. 1A). TALEN mRNA was injected into embryos at the one-cell stage. The injected embryos were raised to adult and the tail genomic DNA was extracted to screen the zebrafish that carried a mutation. A 377bp PCR product containing the TALEN site was amplified and digested with Mlu1 to generate two fragments of 265bp and 112bp in control embryos; the mutations induced by TALEN resulted in these two smaller fragments and the intact 377bp product. The individuals containing mutations were mated with wild-type (WT) zebrafish to obtain the heterozygous mutant zebrafish. With the sequence analysis of the heterozygous mutant zebrafish, 3 insertion or deletion mutations were identified in *CERKL* cDNA (Supplementary Material, Table S1). The 7bp deletion c.43_49delTGGTCGG in *CERKL* gene caused a frame shift resulting in an abnormal p.Trp15Argfs*21 CERKL protein (Fig. 1B). After obtaining this homozygous mutation line, we measured the expression of *CERKL*. We found that the mRNA level of *CERKL* did not change (Fig. 1C), but the CERKL protein was undetectable in the *CERKL*$^{-/-}$ zebrafish (Fig. 1D, Supplementary Material, Fig. S1).

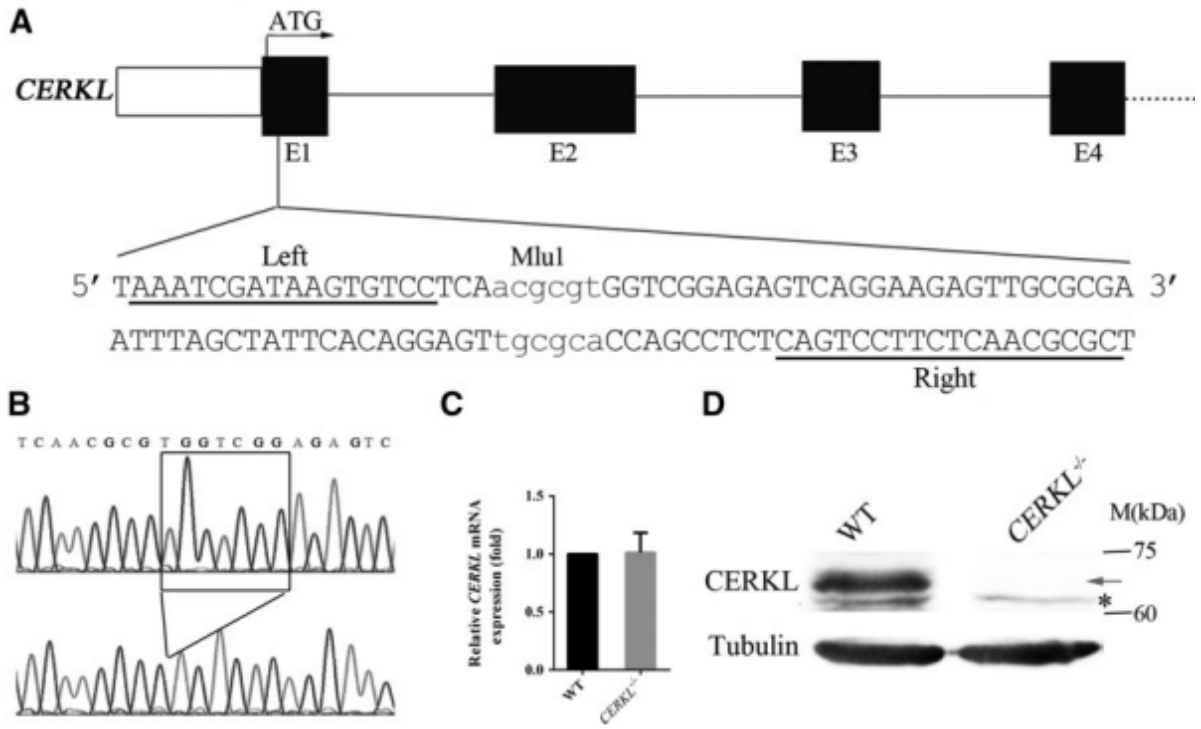

Figure 1 Targeted and heritable disruption of *CERKL* gene in zebrafish. (**A**) The four exons and partial sequence of *CERKL* gene are shown. Left and right TALENs are underlined. The Mlu1 restriction site in the spacer region is used for mutation detection. E1-E4, exon1-exon4. (**B**) Sequencing validation of the c.43_49delTGGTCGG mutation lines. The 7-bp deletion is indicated with a box. (**C**) Detection of the level of *CERKL* mRNA in 4-month-old *CERKL*$^{-/-}$ and WT zebrafish by qRT-PCR. The results are shown as mean ± SD. (**D**) CERKL protein levels of WT and *CERKL*$^{-/-}$ zebrafish at 9M were detected by western blot. The CERKL band marked by arrow is undetectable in *CERKL*$^{-/-}$ zebrafish. The asterisk indicates the non-specific band.

CERKL$^{-/-}$ mutants showed diminished light response at an early stage

Although *CERKL* is highly expressed in several organs, no gross abnormality was observed in our *CERKL*$^{-/-}$ animals. The retina developed normally. Because of the anticipated phenotype, we tested visual function by measuring the electroretinogram (ERG) of *CERKL*$^{-/-}$zebrafish. A typical ERG waveform features three components: an initial negative a-wave originating from photoreceptor activity, a large positive b-wave reflecting mainly ON bipolar cell depolarization and, when longer flashes of light are used, a d-wave reflecting the activity of OFF-bipolar cells and photoreceptors (21,22). Because of an overlap with the b-wave, the a-wave appears small in this ERG measurement (23). 5- to 7-day-old *CERKL*$^{-/-}$zebrafish exhibited a significantly reduced light response (Fig. 2A). The b wave amplitude in *CERKL*$^{-/-}$ zebrafish was reduced by 30% compared with that of control (Fig. 2B), indicating that deletion of *CERKL* affected visual function at an early stage.

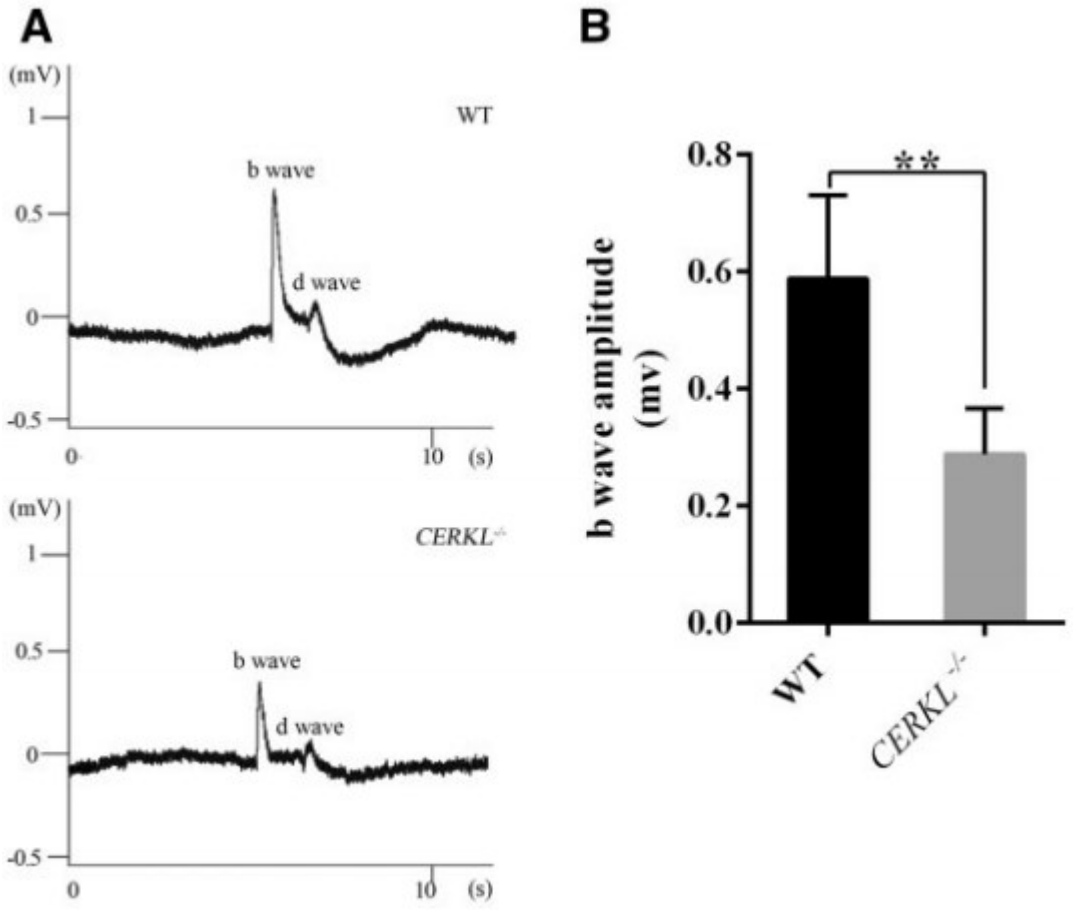

Figure 2 Mild visual impairment in the *CERKL*$^{-/-}$ larvae detected by ERG analysis. (**A**) Representative traces of ERG of WT and *CERKL*$^{-/-}$ zebrafish at 7 dpf. (**B**) Comparison of b-wave amplitudes of WT ($n = 9$) and *CERKL*$^{-/-}$ ($n = 11$) zebrafish using two-tailed Student's *t*-test. The results are shown as mean ± SD. **, $P < 0.01$.

CERKL$^{-/-}$ zebrafish showed a progressive degeneration of the outer retina

CERKL is a rare cause of recessive RP, but the *CERKL*$^{-/-}$ mice model did not show any gross histological changes in the retina. In order to investigate if the *CERKL*$^{-/-}$ zebrafish exhibited a phenotype similar to RP, histological examination of the retina of *CERKL*$^{-/-}$ zebrafish was carried out at different ages. In 1-month-old *CERKL*$^{-/-}$ zebrafish, longitudinal retinal sections of *CERKL*$^{-/-}$ zebrafish showed no significant changes in the retina compared with control (Fig. 3A). At 2 months of age, although the thickness of the retinal outer layer of *CERKL*$^{-/-}$ zebrafish was similar to that of control, the outer segments of photoreceptors arrangement showed early signs of disorganization (Fig. 3B). Progressive decrease in the thickness of the photoreceptor OSs was observed after 2 months of age. At 4 months of age, the OSs of photoreceptors showed obvious degeneration, appearing shorter than normal (Fig. 3C), whereas there was little or no change in any of the other retinal layers. However, at 12 months of age, both the length of the OSs and the thickness of the ONL of *CERKL*$^{-/-}$ zebrafish showed significant decreases, indicating loss of rod and cone photoreceptors (Fig. 3D).

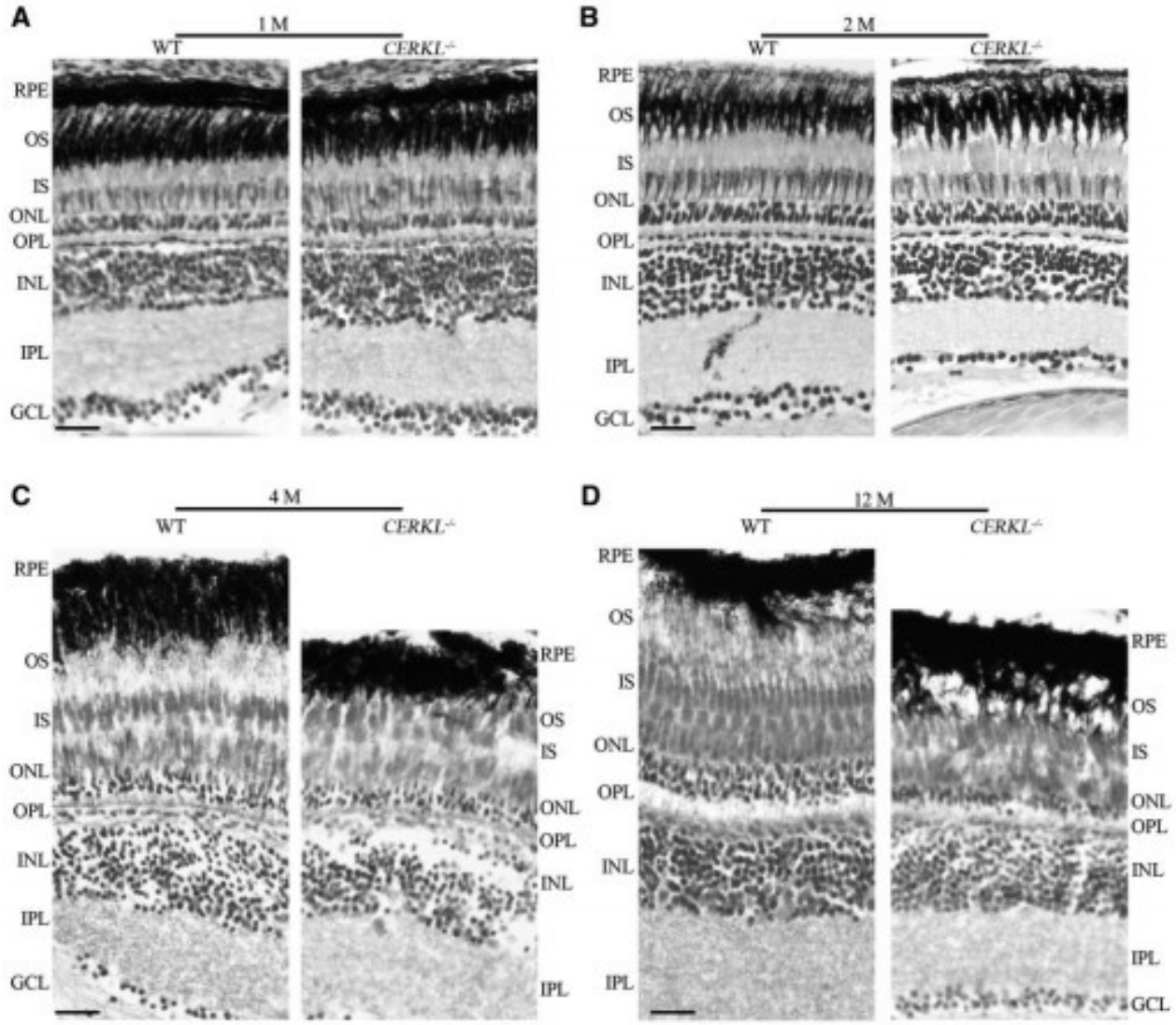

Figure 3*CERKL*$^{-/-}$ zebrafish showed a progressive degeneration of the outer retina. (**A–D**) Histologic analysis of cryosections in *CERKL*$^{-/-}$ and WT zebrafish at indicated ages. RPE, retinal pigment epithelium; OS, outer segment; IS, inner segment; ONL, outer nuclear layer; OPL, outer plexiform layer; INL, inner nuclear layer; IPL, inner plexiform layer; GCL, ganglion cell layer. Scale bars: 20 μm.

Photoreceptor death is a common process in retinal degeneration. Because the morphological results - thinning of the ONL - indicated that the degeneration eventually led to loss of rod and cone photoreceptors in the *CERKL*$^{-/-}$ zebrafish retina, we examined retinal sections from WT and *CERKL*$^{-/-}$ zebrafish, using terminal deoxynucleotidyl transferase dUTP nickend labeling method (TUNEL) and active caspase-3 as markers for cell death. At 12 months of age, when the ONL was significantly reduced, we observed a high number of TUNEL positive photoreceptor and inner nuclear layer nuclei in *CERKL*$^{-/-}$ retinal sections (Fig. 4A and B); in WT zebrafish retina of the same age there were no TUNEL positive signals. Furthermore, compared with the negative signal in WT zebrafish, many active caspase-3 nuclei were observed in the photoreceptor layer (but no other layers) in *CERKL*$^{-/-}$ retina (Fig. 4C and D). The results showed the progressive histological changes in the retina

of *CERKL*$^{-/-}$ zebrafish begin at 2 months, ultimately leading to photoreceptor and inner nuclear layer cell death.

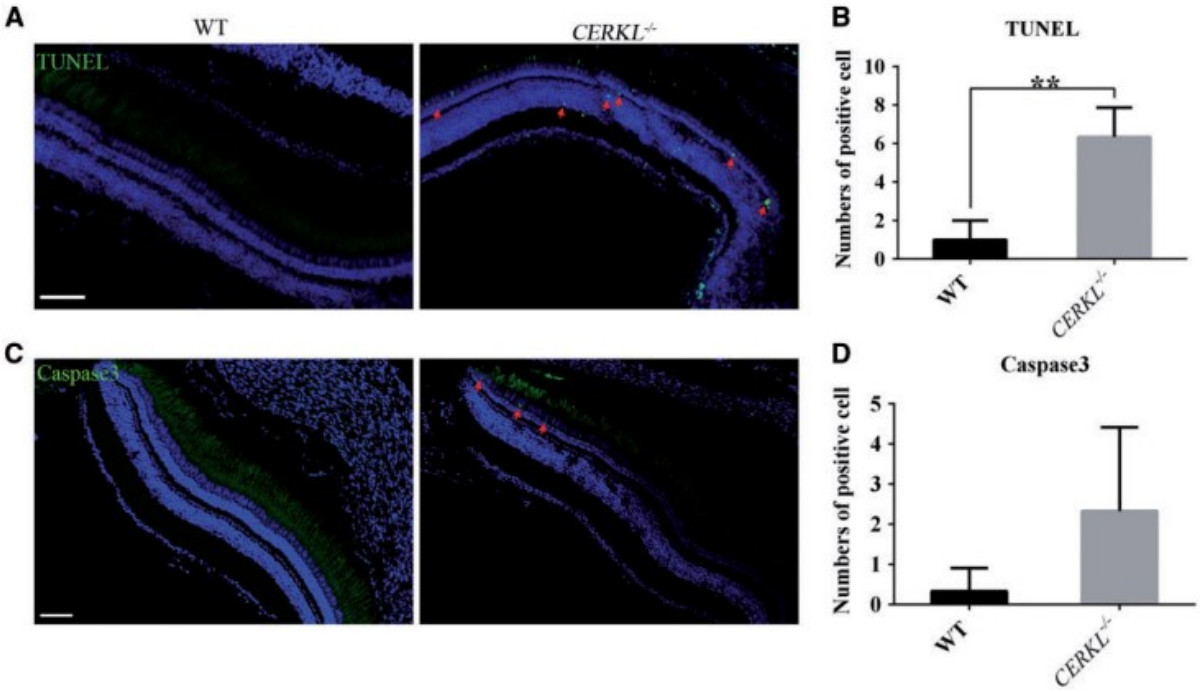

Figure 4 The degeneration of photoreceptors in *CERKL*$^{-/-}$ zebrafish retina was caused by cell death. (**A**) The death of cells was detected by TUNEL. (**B**) Quantification of TUNEL positive cells. The results are shown as mean ± SD. **, $P < 0.01$ (**C**) The apoptotic cells were detected by active caspase-3. (**D**) Quantification of caspase-3 positive cells. The results are shown as mean ± SD. The dead cells are coloured green and the retinal cell nuclei are indicated by DAPI. The red arrow marks the apoptosis cell in the retina. The Scale bars: 50 μm.

CERKL$^{-/-}$ zebrafish exhibited a rod-cone dystrophy phenotype

We extended the morphological studies by analyzing immunofluorescence of retinal frozen sections produced by anti-rhodopsin (4D2) antibody, which labels the rod OSs, and peanut lectin (PNA), which labels the cone OSs. At 1 month of age, no statistically significant difference in the OSs of both rod and cone photoreceptors was detected in *CERKL*$^{-/-}$ zebrafish retina compared to normal control (Fig. 5A and B, top panel). At 2 months of age, *CERKL*$^{-/-}$ retina showed a normal pattern of cone OSs (Fig. 5A, mid-top panel) but disorganized arrangement of rod OSs (Fig. 5B, mid-top panel). By 3 months of age, signs of degeneration in rod OSs were observed, but the length of cone OSs showed no obvious changes (Fig. 5A and B, middle panel). By 7 months of age, degeneration of both rod and cone OSs had ensued, although rod OSs showed more severe damage than did cone OSs (Fig. 5A and B, mid-bottom panel); by the age of 12 months, most OSs of rod and cone photoreceptors of the *CERKL*$^{-/-}$ zebrafish retina had diminished substantially. Moreover, the number of rod and cone photoreceptor nuclei in the ONL decreased significantly from 7 months (Fig. 5A and B, bottom panel). The length of cone and rod OSs at the different ages was statistically analyzed (Fig. 5C and

D). However, immunostaining and western-blot of green (opn1mw) and UV (opn1sw) opsin - which label green and UV cone OS, respectively - showed a normal expression pattern even at the age of 6 months (Supplementary Material, Fig. S2).

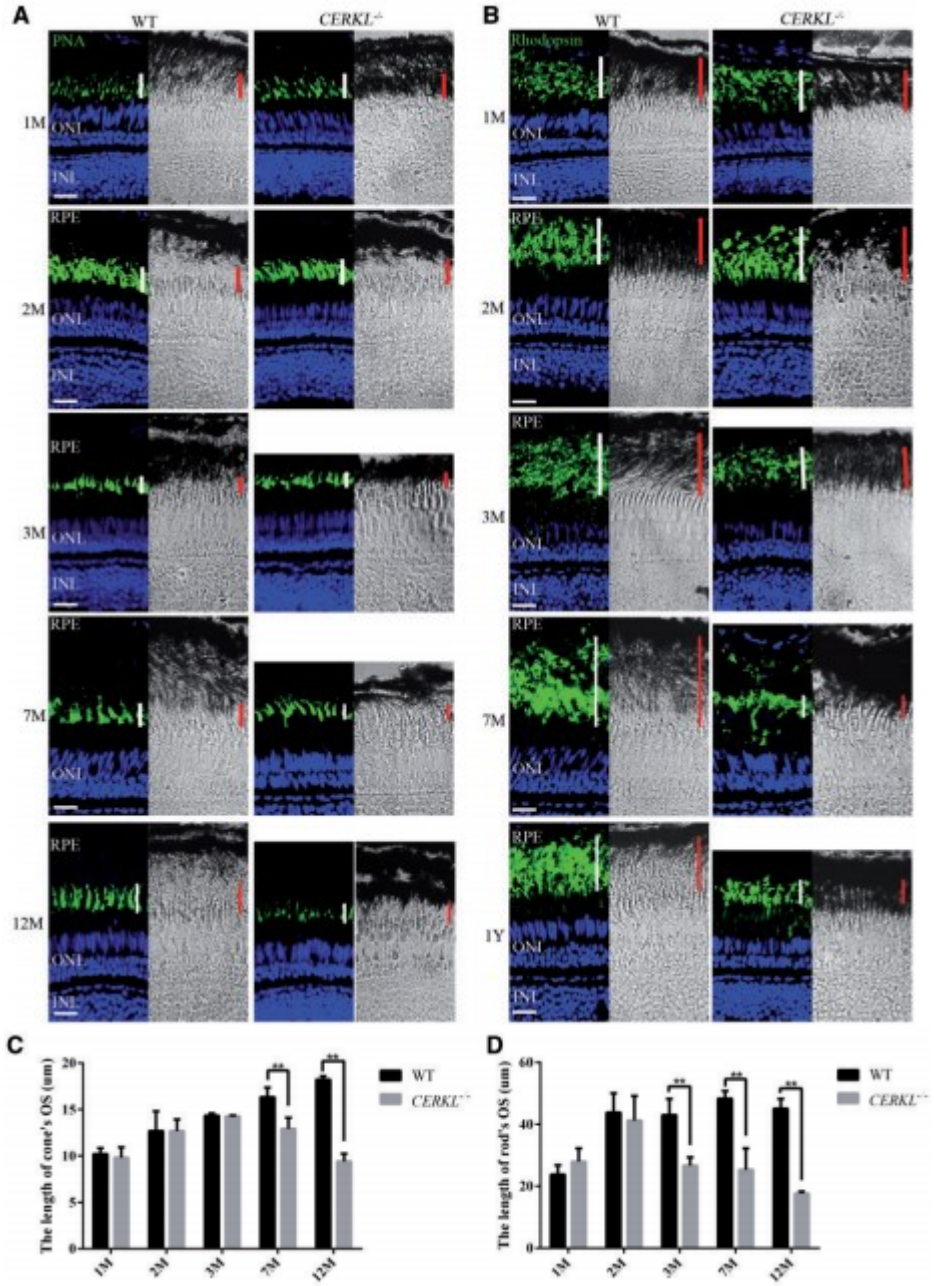

Figure 5 Progressive retinal degeneration involved mainly rod cell death in *CERKL*$^{-/-}$ retinas. Cryosections of *CERKL*$^{-/-}$ and WT zebrafish were stained with PNA (**A**) or rhodopsin (4D2) (**B**) at the indicated ages, highlighting cone or rod photoreceptors, respectively. The white and red lines indicate the thickness of outer segments of cones (A) and rods (B). Scale bars: 20 µm. The length of outer segments of cones (**C**) and rods (**D**) of *CERKL*$^{-/-}$ and WT zebrafish was statistically analyzed. Data are presented as mean ± SD. $^{**}P < 0.01$.

In order to confirm that rod cells were affected prior to cone cells in *CERKL*$^{-/-}$ zebrafish, a number of proteins that express specifically in rod or cone cells were examined at different ages. Rhodopsin,

GRK1, GNAT1 and GNB1 are mainly expressed in rod cells, while GNB3 and GCAP1 are exclusive to cone cells (24). Results from western-blotting showed that in *CERKL*$^{-/-}$ zebrafish the expression of rhodopsin, GRK1, GNAT1 and GNB1 was not changed significantly at age 1 month, but rapid decreases were detected by the age of 2 months; in fact, by age 4 months the rhodopsin was almost undetectable. By contrast, compared with wild type, cone proteins GNB3 and GCAP1 showed no significant changes in *CERKL*$^{-/-}$ zebrafish even at age 4 months (Fig. 6A). The statistical results are shown in Figure 6B. Results from qRT-PCR revealed that most of the genes showed no significant changes at the mRNA level, with the exceptions of Rhodopsin and GNB1B which showed a slight increase (Supplementary Material, Fig. S3).

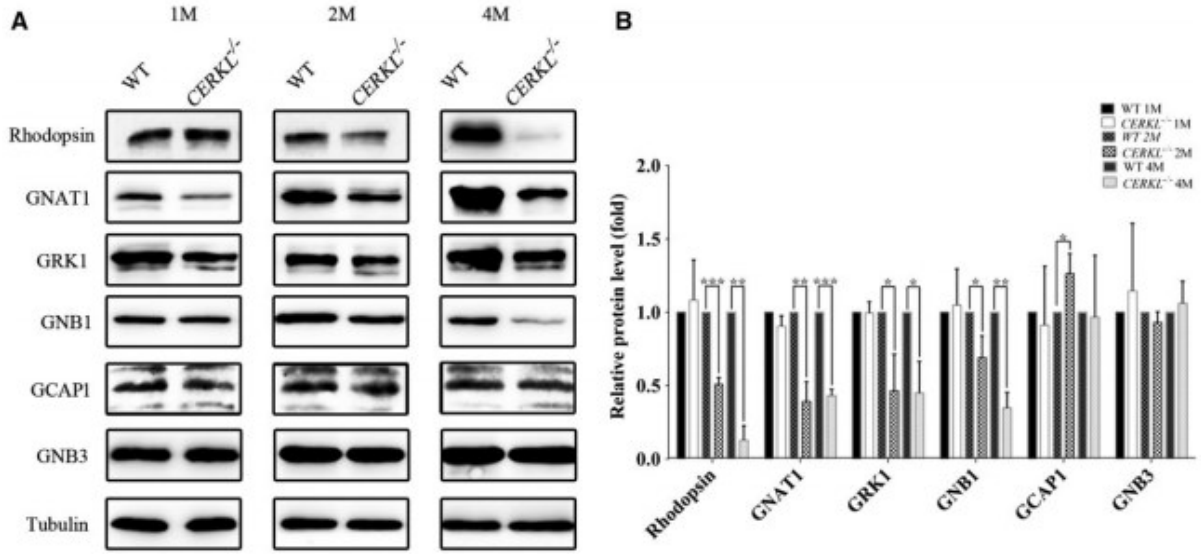

Figure 6 Knockout of *CERKL* resulted in decreased protein levels in rod rather than cone photoreceptors. (**A**) The proteins - rhodopsin, GRK1, GNAT1, GNB1, GNB3 and GCAP1 - were detected by western-blot in wild type and *CERKL*$^{-/-}$ zebrafish. Rhodopsin, GRK1, GNAT1 and GNB1 express specifically in rods, while GNB3 and GCAP1 express specifically in cones. Tubulin acted as an endogenous control. (**B**) Relative protein levels of rhodopsin, GRK1, GNAT1, GNB1, GNB3 and GCAP1. Each experiment was repeated three times and statistical analysis was carried out. Data are presented as mean ± SD. **P* < 0.05, ***P* < 0.01, ****P* < 0.0001.

CERKL knockout caused the interphotoreceptor accumulation of shed OSs

In order to examine the retina at the ultrastructural level, we performed transmission electron microscopic (TEM) analysis of *CERKL*$^{-/-}$ zebrafish retinas at ages 3 and 5 months. TEM results showed that at 3 months of age the most severe signs of degeneration occurred at the OSs near the RPE of *CERKL*$^{-/-}$ zebrafish (Fig. 7B, B') compared with WT (Fig. 7A, A'). The OSs in WT zebrafish retina showed normal morphology and disc stacking (Fig. 7C, C') while disorganized and shortened OSs were observed in many rod photoreceptors of *CERKL*$^{-/-}$ zebrafish, consistent with the findings using light microscopy (Fig. 7D, D').

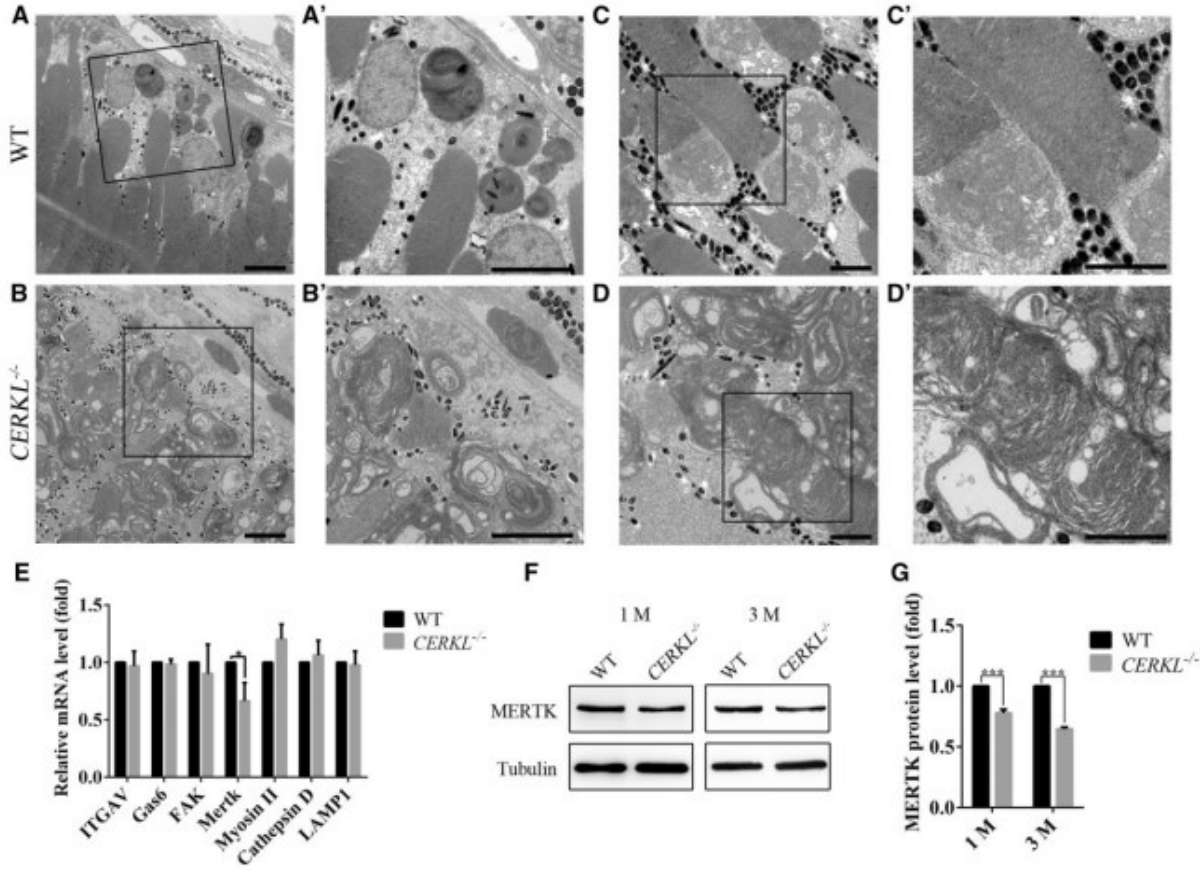

Figure 7 CERKL knockout caused interphotoreceptor accumulation of shed OSs by interfering with the expression of *MERTK*. (**A, A'**) WT zebrafish retina showed well-maintained rod outer segments. (**B, B'**) *CERKL*$^{-/-}$ zebrafish retina confirmed that the most severe degeneration occurred at the rod OS. (**C, C'**) WT zebrafish retina showed normal rod outer segments and inner segments. (**D, D'**) *CERKL*$^{-/-}$ zebrafish showed serious disorganisation in the membranous disc of rod photoreceptor OSs. Scale bars: 1 μm in (A, A', B, B'); 0.25 μm in (C, C', D, D'). (**E**) The mRNA level of phagocytosis associated proteins was detected in 1M *CERKL*$^{-/-}$ and WT zebrafish. Date are presented as mean ± SD. **P* < 0.05. (**F**) The protein level of MERTK was detected in 1M and 3M *CERKL*$^{-/-}$ and WT zebrafish. (G) The quantitative data of at least three independent experiments were statistically analyzed using two-tailed Student's *t*-test. Date are presented as mean ± SD. ****P* < 0.0001.

By the age of 5 months, the defects in *CERKL*$^{-/-}$ zebrafish were more profound: throughout the entire retina the OSs of most rod photoreceptors were detached. Furthermore, a massive accumulation of vesicular structures in the interphotoreceptor spaces was observed in *CERKL*$^{-/-}$ zebrafish (Supplementary Material, Fig. S4B, B'), but not in wild type zebrafish (Supplementary Material, Fig. S4A, A'). These results imply that CERKL may play an important role in OS phagocytosis by the RPE; *CERKL* mutation may lead to defects in photoreceptor outer segment phagocytosis, eventually leading to photoreceptor degeneration.

In order to confirm that dysfunction of phagocytosis occurred in *CERKL*$^{-/-}$ zebrafish larvae, the ultrastructure of rod and cone photoreceptors was examined at 12dpf (days post-fertilization), at

which time some shed OSs and membranous whorls were observed in the interphotoreceptor spaces of *CERKL*$^{-/-}$ (but not WT) retinas. While early phagocytosis deficiency was seen in *CERKL*$^{-/-}$ (but not WT) zebrafish (Supplementary Materials, Fig. S4C, C', D, D'), the OSs of rod and cone photoreceptors in the retinas of *CERKL*$^{-/-}$zebrafish showed no gross histological changes when compared to those of WT retinas.

Deficiency of CERKL leads to dysfunction of RPE phagocytosis and down-regulation of MERTK To explore the underlying mechanism of dysfunction of RPE phagocytosis in *CERKL*$^{-/-}$ zebrafish, phagocytosis-associated protein levels were measured. Given that photoreceptor outer segment phagocytosis by RPE cells requires the coordinated activity of numerous cell surface and cytosolic proteins (25,26), in order to test if knockout of *CERKL* in zebrafish causes a deficiency of phagocytosis, we used qRT-PCR to measure the mRNA levels of several genes involved in photoreceptor recognition, engulfment and degradation in *CERKL*$^{-/-}$ and WT zebrafish at the age of 1 and 3 months. Only MERTK showed decreased mRNA level in 1 month *CERKL*$^{-/-}$ zebrafish compared to WT zebrafish (Fig. 7E). At age 3 months, MERTK showed a further slight decrease in mRNA level. Expression of Cathepsin D and LAMP1 mRNA was also affected (Supplementary Material, Fig. S5).

MERTK plays a key role in RPE phagocytosis: its deficiency causes accumulation of shed OSs and further photoreceptor death (27). Expression of MERTK in the retina of WT and *CERKL*$^{-/-}$ zebrafish at the age of 1 and 3 months was measured by western-blot and was found to be significantly reduced in the *CERKL*$^{-/-}$ retina (Fig. 7F) to 77% and 64% of WT values at 1 and 3 months, respectively (Fig. 7G).

We further investigated the expression of MERTK in *CERKL* knockdown ARPE19 cell line. The interference effects of three different siRNA were detected by qRT-PCR. By contrast with control, the target siCERKL#1 and siCERKL#3 can efficiently decrease the expression of *CERKL* (Fig. 8A, B). Additionally, after knockdown of *CERKL* we observed that the protein and mRNA level of MERTK also decreased significantly (Fig. 8B–D), similar to the results seen in the *CERKL*$^{-/-}$ zebrafish (Fig. 7E–G). To determine whether CERKL functions in OS phagocytosis, we assessed ox-POS ingestion in ARPE19 cells. Control siRNA and siCERKL#1 were transfected into ARPE-19 cells. We found a significant decrease of ox-POS phagocytosis by 41% ($p = 0.0017$) in CERKL siRNA knockdown cells when compared to that of cells transfected with control siRNA (Fig. 8E and F), suggesting a defect of phagocytosis in *CERKL* knockdown cells.

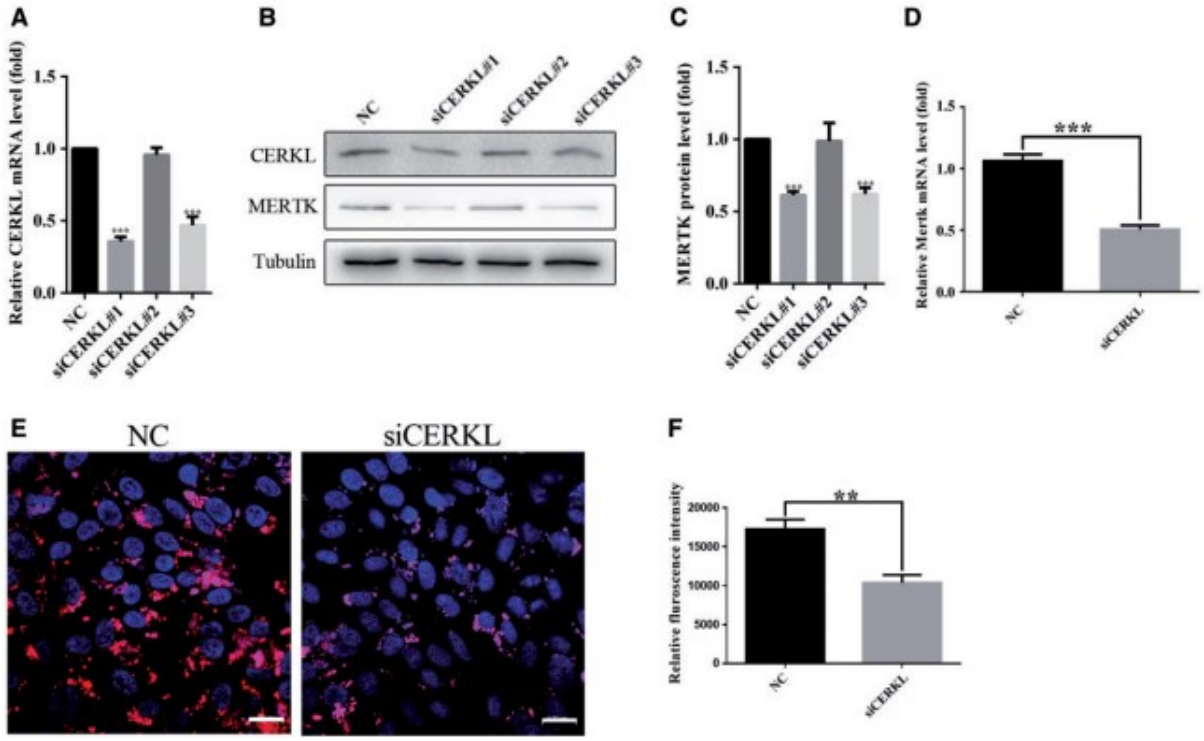

Figure 8 Effect of phagocytosis in CERKL knockdown ARPE19 cells. (**A**) The interference effect of 3 different CERKL target siRNA was examined. After 48h transfection in ARPE-19, the siCERKL#1 and siCERKL#3 decreased the mRNA level of *CERKL* compared with control siRNA. Data are presented as mean ± SD. ***$P < 0.0001$. (**B**) The expression of CERKL and MERTK proteins significantly decreased in siCERKL#1 and siCERKL#3 targeted knockdown ARPE-19 cell line. (**C**) The protein level of MERTK was statistically analyzed using two-tailed Student's *t*-test. Data are presented as mean ± SD. ***$P < 0.0001$. (**D**) The relative *MERTK* mRNA expression showed 53% reduction in siCERKL#1 targeted knockdown ARPE-19 cell line. Data are presented as mean ± SD. ***$P < 0.0001$. (**E**) ARPE19 cells were transfected with control and CERKL siRNA then fed with fluorescence labelled ox-POS. The intracellular fluorescent signals were markedly reduced in CERKL knockdown ARPE19 cells compared to control under confocal microscopy. Scale bars: 20 μm. (**F**) The intracellular fluorescence intensity of ox-POS was measured using Image J software and was found to be significantly decreased by 41% in CERKL knockdown cells. The experiment was done in triplicate and repeated three times. **$P < 0.01$.

Discussion

The phenotype of the *CERKL* knockout zebrafish recapitulated the main features of the clinical signs and symptoms reported in RP patients: progressive retinal degeneration that begins with photoreceptor dysfunction, followed by widespread cell death in all retinal layers (2). More importantly, analysis of *CERKL*$^{-/-}$ zebrafish provided insights regarding several key questions concerning the functions of CERKL.

Patients with mutations in *CERKL* were initially diagnosed as having autosomal recessive RP, which is a form of rod-cone dystrophy. Subsequently, a comprehensive study of the clinical phenotype of RP patients caused by *CERKL* mutation identified early and prominent macular deficits,

leading to the conclusion that *CERKL* mutations are associated with cone-rod dystrophy (2). Although RP is a highly variable disorder, in most forms of the condition the decrease in rod function is more marked than the decrease in cone function; this is consistent with our *CERKL* knockout zebrafish that manifested more rapid degeneration in rods than in cones. Before 2 months of age, there was no significant difference between *CERKL*$^{-/-}$ and WT zebrafish retina, whereas rapid degeneration occurred in *CERKL*$^{-/-}$retinas over 2 months old. The phenotype in the *CERKL*$^{-/-}$ zebrafish was in accordance with that of patients who showed normal development in the first two decades of life, followed by subsequent rapid neurodegeneration (2). Irrespective of the order of photoreceptor degeneration (i.e., rod-cone or cone-rod), *CERKL* mutation-induced phenotypes do not match completely the traditional definition of RP due to the early, prominent macular rod and cone deficits and the relatively severe laminopathy in the late stages of the disease (28). In this study, our results, based on a *CERKL* knockout *in vivo* model, reveal that the degeneration of the rod OSs is earlier and more severe than that of the cone OSs, thus supporting a rod-cone progression in *CERKL* mutant patients.

It has been reported that CERKL interacts with neuronal calcium sensor proteins in the retina (29). Other reports implicated CERKL in light stress (14) and oxidative stress (15). One study proposed that CERKL is an mRNA-binding protein (30). These results suggest that CERKL may have different functions in different types of cells. Although developmental defects additional to retinal deficiencies were observed in *CERKL* knockdown zebrafish (including small heads, markedly curved body axes and short tails) (19), most of the cells that express CERKL were not obviously affected by the deletion of *CERKL*. It may be, then that in most cell types, the loss of the normal CERKL pathway might be compensated by other similar (or parallel) pathways. However, the rod photoreceptors were seriously affected at an early stage of development, suggesting that in rod cells loss of CERKL function cannot be compensated by another similar pathway. A lack of CERKL did not prevent normal development of rod photoreceptors but did result in failure in maintaining the structure and function of the phototransduction apparatus, i.e., expression of key phototransduction cascade proteins and the membrane structure of the OSs where phototransduction takes place.

Since the ERG b-wave in 5-7 dpf zebrafish larvae is determined entirely by cone photoreceptors, it is possible that the early reduction in b-wave amplitude seen in the 5-7 dpf *CERKL*$^{-/-}$ zebrafish larvae may be a consequence of deficits in the phagocytosis of photoreceptor OSs as observed in our TEM results (Supplementary Material, Fig. S4D, D'), although the latter observations were made in older larvae (12 dpf). This reduced cone ERG response in the fish could also have implications for the cone dysfunction observed in patients, despite the lack of cone degeneration at this time point. When expression of photoreceptor cascade proteins was measured, rod-specific expressed proteins such as rhodopsin, GNAT1, GRK1 and GNB1 decreased significantly. More importantly, the decrease occurred between the age of 1 and 2 months when both rod and cone photoreceptor OSs showed no significant signs of cell degeneration. This suggests that the reduction in photoreceptor cascade

proteins was a result of *CERKL* deletion rather than an effect of photoreceptor degeneration. However, there was no change in expression of GNB3 and GCAP1, both of which are cone-specific expressed proteins, even though GCAP1 is known to interact with CERKL. Viewed from this perspective, the primary site of damage of *CERKL*$^{-/-}$ appears to be in the rod OSs. This conclusion leads us to propose that the earliest damage inflicted on rod photoreceptors due to human *CERKL* mutations occurs at the phototransduction level: specifically, by disturbing the structure and function of the phototransduction apparatus.

It is interesting to note that the rod phototransduction cascade protein levels are significantly reduced while the mRNA might remain unchanged at the age of 4 months in our CERKL knockout zebrafish (Fig. 6A and B, Supplementary Material, Fig. S3). It is possible that loss of *CERKL* causes defects in rod phagocytosis and results in detached rod OSs, which degenerate into membranous debris zones and lead to unstable phototransduction cascade protein degradation. The reduced rod protein level might also be due to reduced translation. As CERKL was found to directly interact through its N-terminal region with mRNA and also to bind to some proteins of the translation machinery (30), the loss of CERKL may lead to reduced *de novo* protein synthesis in our zebrafish. CERKL is distributed widely in the retina, expressing in the photoreceptors but also present in the INL, RGL and RPE. Previous studies mainly focused on the function of CERKL in the photoreceptor layer; its function in other retinal layers is unknown. The RPE plays a crucial role in maintaining the survival of photoreceptors, in particular through phagocytosis of shed photoreceptor OSs (31,32). A failure of phagocytosis will result in the degradation of some specific phototransduction proteins and death of photoreceptors (33). Two presumptive consequences of this defective phagocytosis, specifically the formation of membranous whorls adjacent to the RPE surface and longer-than-normal OSs (34), were seen in our *CERKL*$^{-/-}$ zebrafish as early as 12dpf. In the retinas of 3- and 5-month-old *CERKL*$^{-/-}$ zebrafish, we also observed a high degree of interphotoreceptor accumulation of shed OSs, while the expression of MERTK significantly decreased in *CERKL*$^{-/-}$zebrafish. In ARPE19 cells, we also found a significant decrease of ox-POS phagocytosis in CERKL siRNA knock-down cells, as well as in *MERTK* mRNA and protein levels (Fig. 8D–F). These results suggest that CERKL may locate in the RPE and participate in RPE phagocytosis. Future studies may elucidate the molecular mechanism by which *CERKL* deficiency affects the expression of *MERTK* in retina.

Finally, given that vision was diminished in the *CERKL*$^{-/-}$ zebrafish as early as age 1 week while degeneration did not occur until age 8 weeks, this 7-week "presymptomatic" interval may be a window of opportunity to screen for treatment options that might halt or delay disease progression. The zebrafish offers several advantages for eye research, including its transparent embryo that facilitates visualization of developing retinal structures and its amenability to pharmacological screens. The phenotypic features highlighted above make an even more compelling case for the *CERKL*$^{-/-}$ zebrafish model.

Materials and Methods

Zebrafish lines and maintenance

Zebrafish were kept under standard laboratory conditions at 28.5 °C in a 14/10-h light/dark cycle. Fertilized eggs were obtained and grown in E3 medium (5 mM NaCl, 0.17 mM KCl, 0.33mM CaCl2, 0.33 mM MgSO4) at 30 °C incubators. All the procedures were performed in accordance with the ARVO statement for the Use of Animals in Ophthalmic and Vision Research.

Generating *CERKL* mutant by TALENs

TALENs target sites were designed using the online service at: https://tale-nt.cac.cornell.edu/node/add/talen. The sequence-specific TAL effector repeats against the right and left arms were constructed utilizing the FastTALE TALEN kit (Sidansai Biotechnology, Shanghai, China). Templates for mRNA synthesis were linearized by Not1from TALEN expression vectors. mRNA of left and right TALENs were synthesized by the SP6 mMessage mMachine Kit (Ambion, Austin, TX, USA) and purified by Lithium chloride precipitation. The left and right TALEN mRNA were mixed at the ratio of 1:1 and co-injected into wild-type zebrafish embryos at one cell stage at a final concentration of 100 ng/μl each. To evaluate the efficiency of the generated TALEN, the genomic DNA of a total of 30 injected and normally developing embryos at 2dpf were extracted followed by PCR amplification. A 377bp DNA fragment containing the *CERKL* target site was amplified by PCR (5'-TTCCTCAAGAGCCTAGCGAC-3', 5'-TGTTACCCGCGTTGTCGTAA-3'), which were then digested by Mlu1. The digested products were separated by 2% agarose gel electrophoresis. To identify the mutation of their offspring, the F0 embryos were raised to adulthood and outcrossed with wild-type zebrafish. The F1 embryos were collected for genomic DNA extraction and digested by Mlu1 as described above.

HE staining and immunofluorescence

Eyecups dissected from adult zebrafish or zebrafish embryos were fixed in 4% paraformaldehyde (PFA). For cryosections, adult or embryo eyecups were dehydrated in 30% sucrose at 4 °C overnight and embedded in O.C.T. Cryosections of adult eyecups were haematoxylin and eosin stained under standard conditions. For immunofluorescence, slides containing sections were incubated with PDT (PBS/1%DMSO/0.1%Triton) for 10min and blocked with blocking solution (PDT/1%BSA/10%goat serum). The following primary antibodies were used: mouse anti 4D2 conjugated FITC 1:200 (Abcam, Cambridge, MA, USA), rabbit anti-opn1mw (green) (ABclonal, Custom), rabbit anti-op1sw (uv) (ABclonal, Custom) and rabbit anti-caspase3 1:100 (BD Bioscience, San Jose, CA, USA) were incubated in primary antibody dilution (PDT/1%BSA/2%goat serum) while Peanut agglutinin (PNA) conjugated to Alexa Fluor 488 (5 mg/ml; Life Technologies, Carlsbad, CA, USA) were incubated in PBS at 4 °C overnight. Secondary antibodies, Alexa Fluor 488 goat anti-rabbit immunoglobulin G or Alexa Fluor 594 goat anti-mouse immunoglobulin G (Life Technologies) were diluted in PBDT (PDT/1%BSA) and incubated in 37 °C for 1 h. Nuclei were stained with DAPI (Invitrogen™|Life

Technologies). For TUNEL assay, an *in situ* cell death detection kit conjugated with tetra-methyl-rhodamine or fluorescein isothiocyanate (Roche Diagnostics, Mannheim, Germany) was used according to the manufacturer's instructions after pretreatment with proteinase K. Images were captured using an OLYMPUS FV1000 Viewer confocal microscope.

RNA isolation and RT-PCR

Total RNA of zebrafish eyecups or ARPE19 cells was extracted using Trizol (Invitrogen™|Life Technologies), and quantitated by NanoDrop spectrometry (Thermo Scientific, Wilmington, DE, USA). cDNA was generated by MMLV reverse transcriptase (Invitrogen™|Life Technologies). qRT-PCR was performed using AceQ® qPCR SYBR® Green Master Mix (Vazyme, Nanjing, Jiangsu, China) according to the manufacturer's instructions and relative gene expression was quantified using the StepOnePlusTM Real-Time PCR System (Life Technologies). Gene primers used are listed in Supplementary Material, Table S2.

Western blotting

Adult zebrafish eyecups were isolated and homogenized in cold RIPA buffer supplemented with protease inhibitor cocktail (Roche). Protein concentrations were determined by the BCA Protein Assay Kit (Beyotime Biotechnology, Shanghai, China). Ten micrograms of total proteins were separated on a 12% PAGE gel under denaturing conditions and immunoblotting onto NC membranes. Membranes were then blocked in 5% nonfat milk solution in TBST for 1 h at room temperature followed by incubation with primary antibody, mouse anti-rhodopsin (4D2) 1:1000 (Abcam), rabbit anti-GNB1 1:1000 (Abgent Biotech, San Diego, CA, USA), rabbit anti-GNB3 1:1000 (ProteinTech), rabbit anti-GRK1 1:500 (ABclonal, Cambridge, MA, USA), rabbit anti-GNAT1 1:500 (ABclonal), rabbit anti-GCAP1 1:1000 (ProteinTech), rabbit anti-Mertk 1:1000 (Novus Biologicals, Littleton, CO), rabbit anti-CERKL (ABclonal, Custom) at 4 °C overnight. After washing with TBST, membranes were incubated with horseradish peroxidase-conjugated goat anti-rabbit or anti-mouse IgG secondary antibody in TBST (1:20000) and visualized using ChemiDocTM XRS+ system (BIO-RAD).

Transmission electron microscopy (TEM)

For TEM, zebrafish eyes were isolated and fixed in 4% PFA and 2.5% glutaraldehyde in PBS for 1 h at RT. After removing the lens and cornea, the retinas were postfixed in the same fixative solution for 1 h. After three washes with PBS, the retina was fixed again in 2% osmium tetraoxide and dehydrated through an ethanol gradient followed by treatment with propylene oxide and embedded in epoxy resin. Ultrathin sections were prepared using an ultramicrotome to obtain 1-μm-thick sections. Specimens were visualized with a transmission electron microscope (HT7700, Hitachi, Japan).

Phagocytosis assay

Photoreceptor outer segments (POS) were prepared from bovine retina. The prepared POS were oxidized through exposure to a 302 nm ultraviolet light for 18 h. The oxidized-POS (ox-POS) were labelled with CellTracker™ Dye (Thermo Fisher Scientific) following the manufacturer's protocol.

ARPE19 cells were seeded on coverslips in 12-well plates and transfected with control and CERKL siRNA. After 48 h, cells were treated with ox-POS (1 × 106/ml) for 4 h, then washed five times with PBS and fixed with 4% PFA for 10 min at room temperature. The fixed cells were mounted with Vectashield medium containing DAPI (Vector Lab Ltd. Peterborough, UK). The phagocytosed ox-POS were visualized under LSM 510 Zeiss confocal microscope (Zeiss). The fluorescence intensity in treated and untreated ARPE19 cells was quantified using Image J software.

Acknowledgement

X.S. was supported by the Rosetrees Trust, UK Fight for Sight and National Eye Research Center.

Conflict of Interest statement. None declared.

Funding

National Natural Science Foundation of China (No. 81371064, 31571303, 31471199, 81500762, 31601026 and 81670890), Research Fund for the Doctoral Program of Higher Education of China (20120142110077), Rosetrees Trust, UK Fight for Sight and National Eye Research Center.

References

1 Tuson M., Marfany G., Gonzalez-Duarte R. (2004) Mutation of CERKL, a novel human ceramide kinase gene, causes autosomal recessive retinitis pigmentosa (RP26). *Am. J. Hum. Genet*., 74, 128–138.

2 Aleman T.S., Soumittra N., Cideciyan A.V., Sumaroka A.M., Ramprasad V.L., Herrera W., Windsor E.A., Schwartz S.B., Russell R.C., Roman A.J. et al. (2009) CERKL mutations cause an autosomal recessive cone-rod dystrophy with inner retinopathy. *Invest. Ophthalmol. Vis. Sci*., 50, 5944–5954.

3 Littink K.W., Koenekoop R.K., van den Born L.I., Collin R.W., Moruz L., Veltman J.A., Roosing S., Zonneveld M.N., Omar A., Darvish M. et al. (2010) Homozygosity mapping in patients with cone-rod dystrophy: novel mutations and clinical characterizations. *Invest. Ophthalmol. Vis. Sci*., 51, 5943–5951.

4 Auslender N., Sharon D., Abbasi A.H., Garzozi H.J., Banin E., Ben-Yosef T. (2007) A common founder mutation of CERKL underlies autosomal recessive retinal degeneration with early macular involvement among Yemenite Jews. *Invest. Ophthalmol. Vis. Sci* ., 48, 5431–5438.

5 Ali M., Ramprasad V.L., Soumittra N., Mohamed M.D., Jafri H., Rashid Y., Danciger M., McKibbin M., Kumaramanickavel G., Inglehearn C.F. (2008) A missense mutation in the nuclear localization signal sequence of CERKL (p.R106S) causes autosomal recessive retinal degeneration. *Mol. Vis*., 14, 1960–1964.

6 Abu-Safieh L., Alrashed M., Anazi S., Alkuraya H., Khan A.O., Al-Owain M., Al-Zahrani J., Al-Abdi L., Hashem M., Al-Tarimi S. et al. (2013) Autozygome-guided exome sequencing in retinal dystrophy patients reveals pathogenetic mutations and novel candidate disease genes. *Genome Res*.,

23, 236–247.

7 Avila-Fernandez A., Riveiro-Alvarez R., Vallespin E., Wilke R., Tapias I., Cantalapiedra D., Aguirre-Lamban J., Gimenez A., Trujillo-Tiebas M.J., Ayuso C. (2008) CERKL mutations and associated phenotypes in seven Spanish families with autosomal recessive retinitis pigmentosa.

Invest. Ophthalmol. Vis. Sci., 49, 2709–2713.

8 Tang Z., Wang Z., Wang Z., Ke T., Wang Q.K., Liu M. (2009) Novel compound heterozygous mutations in CERKL cause autosomal recessive retinitis pigmentosa in a nonconsanguineous Chinese family. *Arch. Ophthalmol*., 127, 1077–1078.

9 Khan A.O., Abu-Safieh L. (2014) Rod-cone dystrophy with initially preserved visual acuity despite early macular involvement suggests recessive CERKL mutations. *Ophthalmic Genet*, 36, 369–372.

10 Bornancin F., Mechtcheriakova D., Stora S., Graf C., Wlachos A., Devay P. Urtz N., Baumruker T., Billich A. (2005) Characterization of a ceramide kinase-like protein. *Biochim. Biophys. Acta*, 1687, 31–43.

11 Graf C., Niwa S., Muller M., Kinzel B., Bornancin F. (2008) Wild-type levels of ceramide and ceramide-1-phosphate in the retina of ceramide kinase-like-deficient mice. *Biochem. Biophys. Res. Commun*., 373, 159–163.

12 Inagaki Y., Mitsutake S., Igarashi Y. (2006) Identification of a nuclear localization signal in the retinitis pigmentosa-mutated RP26 protein, ceramide kinase-like protein. *Biochem. Biophys. Res. Commun*., 343, 982–987.

13 Tuson M., Garanto A., Gonzalez-Duarte R., Marfany G. (2009) Overexpression of CERKL, a gene responsible for retinitis pigmentosa in humans, protects cells from apoptosis induced by oxidative stress. *Mol. Vis*., 15, 168–180.

14 Mandal N.A., Tran J.T., Saadi A., Rahman A.K., Huynh T.P., Klein W.H., Cho J.H. (2013)

Expression and localization of CERKL in the mammalian retina, its response to light-stress, and relationship with NeuroD1 gene. *Exp. Eye Res*., 106, 24–33.

15 Li C., Wang L., Zhang J., Huang M., Wong F., Liu X., Liu F., Cui X., Yang G., Chen J. et al. (2014) CERKL interacts with mitochondrial TRX2 and protects retinal cells from oxidative stress-induced apoptosis. *Biochim. Biophys. Acta*, 1842, 1121–1129.

16 Garanto A., Vicente-Tejedor J., Riera M., de la Villa P., Gonzalez-Duarte R., Blanco R., Marfany

G. (2012) Targeted knockdown of Cerkl, a retinal dystrophy gene, causes mild affectation of the retinal ganglion cell layer. *Biochim. Biophys. Acta*, 1822, 1258–1269.

17 Garanto A., Riera M., Pomares E., Permanyer J., de Castro-Miro M., Sava F., Abril J.F., Marfany

G., Gonzalez-Duarte R. (2011) High transcriptional complexity of the retinitis pigmentosa CERKL gene in human and mouse. *Invest. Ophthalmol. Vis. Sci*., 52, 5202–5214.

18 Lieschke G.J., Currie P.D. (2007) Animal models of human disease: zebrafish swim into view.

Nat. Rev. Genet ., 8, 353–367.

19 Riera M., Burguera D., Garcia-Fernandez J., Gonzalez-Duarte R. (2013) CERKL knockdown causes retinal degeneration in zebrafish. *PLoS One*, 8, e64048.

20 Huang P., Xiao A., Zhou M., Zhu Z., Lin S., Zhang B. (2011) Heritable gene targeting in zebrafish using customized TALENs. *Nat. Biotechnol*., 29, 699–700.

21 Makhankov Y.V., Rinner O., Neuhauss S.C. (2004) An inexpensive device for non-invasive electroretinography in small aquatic vertebrates. *J. Neurosci. Methods*, 135, 205–210.

22 Kainz P.M., Adolph A.R., Wong K.Y., Dowling J.E. (2003) Lazy eyes zebrafish mutation affects Muller glial cells, compromising photoreceptor function and causing partial blindness. *J Comp Neurol*., 463, 265–280.

23 Avanesov A., Malicki J. (2010) Analysis of the retina in the zebrafish model. *Methods Cell Biol*., 100, 153–204.

24 Lamb T.D. (2013) Evolution of phototransduction, vertebrate photoreceptors and retina.

Prog. Retin. Eye Res., 36, 52–119.

25 Mazzoni F., Safa H., Finnemann S.C. (2014) Understanding photoreceptor outer segment phagocytosis: use and utility of RPE cells in culture. *Exp. Eye Res*., 126, 51–60.

26 Kevany B.M., Palczewski K. (2010) Phagocytosis of retinal rod and cone photoreceptors.

Physiology (Bethesda), 25, 8–15.

27 Feng W., Yasumura D., Matthes M.T., LaVail M.M., Vollrath D. (2002) Mertk triggers uptake of photoreceptor outer segments during phagocytosis by cultured retinal pigment epithelial cells. *J. Biol. Chem*., 277, 17016–17022.

28 Hartong D.T., Berson E.L., Dryja T.P. (2006) Retinitis pigmentosa. *Lance* , 368, 1795–1809.

29 Nevet M.J., Vekslin S., Dizhoor A.M., Olshevskaya E.V., Tidhar R., Futerman A.H., Ben-Yosef T.

(2012) Ceramide kinase-like (CERKL) interacts with neuronal calcium sensor proteins in the retina in a cation-dependent manner. *Invest. Ophthalmol. Vis. Sci*., 53, 4565–4574.

30 Fathinajafabadi A., Perez-Jimenez E., Riera M., Knecht E., Gonzalez-Duarte R. (2014) CERKL, a retinal disease gene, encodes an mRNA-binding protein that localizes in compact and untranslated mRNPs associated with microtubules. *PLoS One*, 9, e87898.

31 Strauss O. (2005) The retinal pigment epithelium in visual function. *Physiol. Rev*., 85, 845–881.

32 Young R.W. (1967) The renewal of photoreceptor cell outer segments. *J. Cell Biol*., 33, 61–72.

33 Cook B., Lewis G.P., Fisher S.K., Adler R. (1995) Apoptotic photoreceptor degeneration in experimental retinal detachment. *Invest. Ophthalmol. Vis. Sci*., 36, 990–996.

34 Duncan J.L., LaVail M.M., Yasumura D., Matthes M.T., Yang H., Trautmann N., Chappelow

A.V., Feng W., Earp H.S., Matsushima G.K. et al. (2003) An RCS-like retinal dystrophy phenotype in mer knockout mice. *Invest. Ophthalmol. Vis. Sci*., 44, 826–838.